JOURNAL OF GEOPHYSICAL RESEARCH, VOL. 87, NO. A4, PAGES 2525–2532, APRIL 1, 1982

The Electron Content and Its Variations at Natal, Brazil

T. R. TYAGI,[1] K. C. YEH,[2] AND A. TAURIAINEN[3]

Department of Electrical Engineering, University of Illinois at Urbana-Champaign Urbana, Illinois 61801

H. SOICHER

Center for Communication Systems, U.S. Army Communication Research and Development Command Fort Monmouth, New Jersey 07703

The Faraday rotation and amplitude data for the period September 1978 through August 1979, recorded from the geostationary satellite SMS 1 (90°W) at Natal (5.9°S, 35.2°W), have been utilized to study the behavior of total electron content (TEC). Apart from diurnal and seasonal behavior of TEC, two characteristic features of the nighttime ionosphere are discussed: (1) a postsunset enhancement in TEC which lasts for several hours following the rapid sunset decrease and (2) the sharp, isolated changes in TEC. In particular, relating to phenomenon 2, the depletions in TEC are usually accompanied by a simultaneous increase in fading rate, scintillation index, and amplitude level, while the enhancements are accompanied by a simultaneous decrease in fading rate, scintillation index, and amplitude level. The statistics of their occurrence and nature are described. The average behavior of the signal amplitude after propagating through either a depleted or an enhanced ionosphere is modeled theoretically and shown to be in agreement with the observed experimental behavior.

BEHAVIOR OF TOTAL ELECTRON CONTENT (TEC) AT NATAL

Diurnal and Seasonal Variation in TEC

Natal is an equatorial station (latitude 5.9°S, dip −9.6°). A rotation of π rad on the 136.379-MHz signal received from the geostationary satellite SMS 1 (90°W) is equivalent to 1.89 $\times 10^{17}$ el/m^2 in total electron content for a mean field height of 350 km. To study the general behavior of TEC in different seasons, 10–12 days of uninterrupted data were selected from the periods September–October 1978, December 1978 to January 1979, March–April 1979, and June–July 1979. The hourly median values of TEC are plotted in Figure 1. It may be pointed out here that no claims are made regarding the absolute value of the TEC, especially for individual cases near the diurnal minimum values, for want of independent calibration. It is, however, felt that the error in the median values is only a small fraction of π and that no $n\pi$ ambiguity is involved, though it may sometimes be present in indivdual day-to-day values.

Diurnally, the minimum occur around 0500 hours LMT in all the seasons, while the maximum occurs around 1500 LMT in the June solstice (winter), 1200 LMT in the December solstice (summer), 1330 LMT in the spring equinox, and 1430 LMT in the fall equinox. The electron content increases rapidly following sunrise. The rate of increase is very fast during spring, fall, and the December solstice but very slow during the June solstice. After attaining the diurnal maximum value the electron content decreases very fast during spring, fall, and the June solstice but rather slowly during the December solstice. The average diurnal minimum and maximum values of TEC for spring, fall, winter, and summer are 1.33×10^{17} and 9.07×10^{17}, 1.11×10^{17} and 11.47×10^{17}, 0.67×10^{17} and 5.70×10^{17}, and 1.00×10^{17} and 7.94×10^{17} m^{-2} respectively, giving a diurnal ratio of TEC of 6.8, 10.5, 8.8, and 7.9. It may be noted that, in general, the decay rate of the TEC after sunset is greater than the buildup rate at sunrise.

Postsunset Enhancement in TEC

Following the dramatic drop in Faraday rotation angle for an hour or so after sunset, it may then either settle down to a gradual decay, finally reaching a minimum just before the following sunrise, or sometimes, and at different seasons, a substantial increase in TEC occurs for a duration of 3–4 hours centered around 2300 LMT. This phenomenon is much more pronounced during equinoxes and hence is very visible even in median curves, while only a trace increase is noticeable in solstices. On the evening of November 25, 1978, as shown in Figure 2, the increase at 2200 LMT is approximately 1.65π rad or 3.12×10^{17} el/m^2, which is nearly one half of the diurnal variation, while on the night of November 15, 1978, the increase at 2230 LMT is 3.8π radians or 7.18×10^{17} el/m^2, which is about 90% of the diurnal maximum and about 4% more than the diurnal change in TEC (Figure 3). This nocturnal increase, in varying degrees, has been observed both on days of no scintillation as well as on days of strong scintillation. Therefore it is not likely to be connected with the irregularity-producing mechanism.

The large postsunset enhancements in equatorial zone have been reported by various workers [e.g., *Hunter*, 1969; *Koster*, 1972; *Koster and Beer*, 1972; *Yeboah-Amankwah and Koster*, 1972; *Donatelli et al.*, 1981]. It was suggested that the *F* region dynamo theory [*Rishbeth*, 1971, 1977] may offer the most plausible explanation for this effect. *Rishbeth* [1971, 1977] suggested that the neutral winds in the *F* region produce polarization fields that short-circuit through the *E*

[1] On leave from National Physical Laboratory, New Delhi 110012, India.
[2] Now visiting National Sun Yat-sen University, Kaoshiung, Taiwan 800, Republic of China.
[3] On leave from the University of Oulu, 90570 Oulu 57, Finland.

Paper number 2A0027.
0148-0227/82/002A-0027$02.00

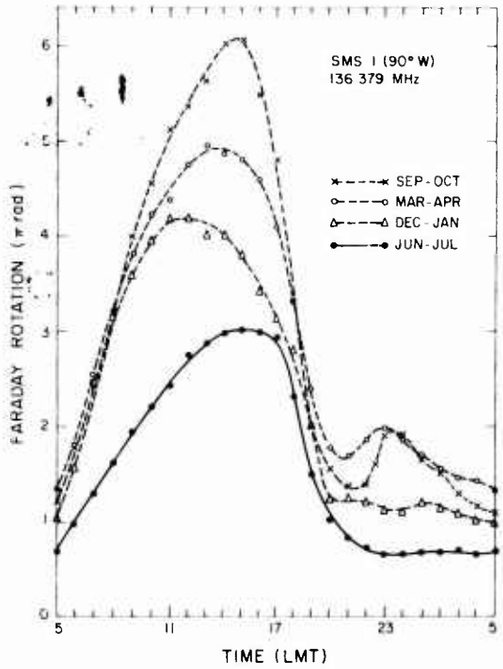

Fig. 1. Diurnal and seasonal variation of TEC over Natal, Brazil, for the period September 1978 through August 1979.

region in daytime but build up at sunset through the sudden drop in E region conductivity. This produces large upward drifts, resulting in a rapid lifting of the F layer and massive transport of plasma along field lines. The rapid lifting causes an artificial apparent decrease in the total Faraday rotation because the layer is carried to higher altitudes at which the magnetic field is weaker, and in addition, the upward transport causes a real physical decrease in the vertical columnar TEC at the equator over and above that expected from the artificial decrease alone. The combined effects of these mechanisms result in a rapid sunset decline in Faraday rotation as noted by *Koster* [1972] with a dip latitude of 4°. This effect is quite pronounced in the present observations from Natal, less pronounced in *Hunter*'s [1969] observations

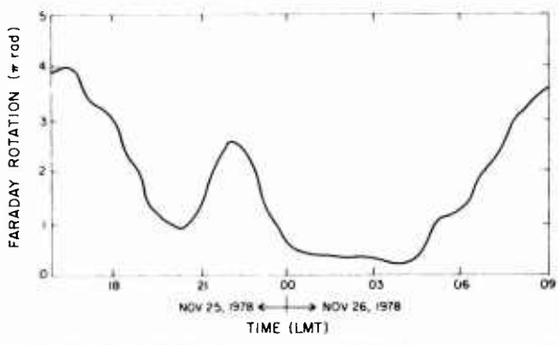

Fig. 2. Typical Faraday rotation variation showing postsunset enhancement as observed on November 25, 1978. This day is marked by the absence of scintillation even though scintillations are usually very active in November.

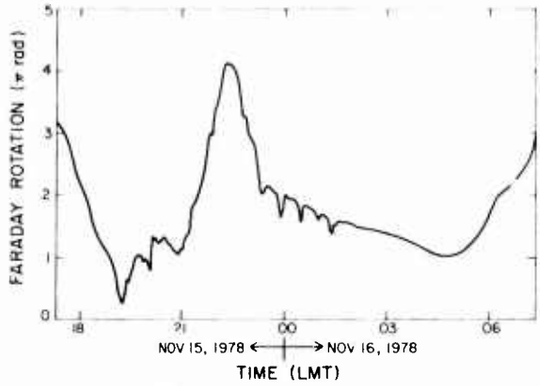

Fig. 3. Typical Faraday rotation variation showing sharp, isolated depletions superposed over the enhancements in the period 2100–2330 as well as the normal decaying nighttime ionosphere after local midnight.

at 13° dip latitude, and even less in the Ascension Island observations [*Donatelli et al.*, 1981] at 15° dip latitude. These observations are consistent with the Defense Meteorological Satellite Program measurements in the postsunset (1930 LT) sector at 840 km which showed smooth density depletions in the immediate vicinity of the magnetic equator with enhancements in the ±10°–20° magnetic latitude range. The subsequent increase around local midnight in TEC, however, is more pronounced in the present and in Hunter's observations.

We note that the above arguments [cf. *Koster*, 1972] clearly explain the dramatic decrease in TEC after sunset at the magnetic equator and the relative increase in electron density in the 10°–20° magnetic latitude range, but the very large enhancements in TEC around 2200–2300 LT in the equatorial ionosphere as reported in this paper are not explicitly explained. *Lanzerotti et al.* [1976] reported, discussed, and related the occurrence of nighttime ledges in TEC measurements at Arecibo, via a model calculation, to the rise and fall of the height of the F_2 peak around midnight. They concluded that the characteristics of the nighttime ledge observed at Arecibo could be directly related to the meridional component of nighttime thermospheric winds. *Anderson and Roble* [1974] studied the behavior of the nighttime ionosphere near the geomagnetic equator and showed that the $\mathbf{E} \times \mathbf{B}$ vertical drifts can cause perturbations in the neutral winds and temperatures. Recently, *Bittencourt and Sahai* [1979], using a tropical ionospheric F region model described by *Bittencourt and Tinsley* [1976], investigated the effect of $\mathbf{E} \times \mathbf{B}$ drift velocity on the local time dependence of N_mF_2, h_mF_2, and 6300-Å emission at the magnetic equator. They concluded that the times of N_mF_2 enhancements during the night are closely related to the time history of the vertical $\mathbf{E} \times \mathbf{B}$ drift, its magnitude, and time of reversal. When the postsunset enhancement in upward drift is well developed and downward drift commences after 2000 LT, then N_mF_2 enhancement occurs around 0200 LT. When upward drift is less pronounced and downward drift occurs at 1900 LT, the enhancement occurs around 2230 LT [cf. *Bittencourt and Sahai*, 1979; *Anderson and Rusch*, 1980]. This clearly explains the variability of TEC enhancements during the nighttime at equatorial stations.

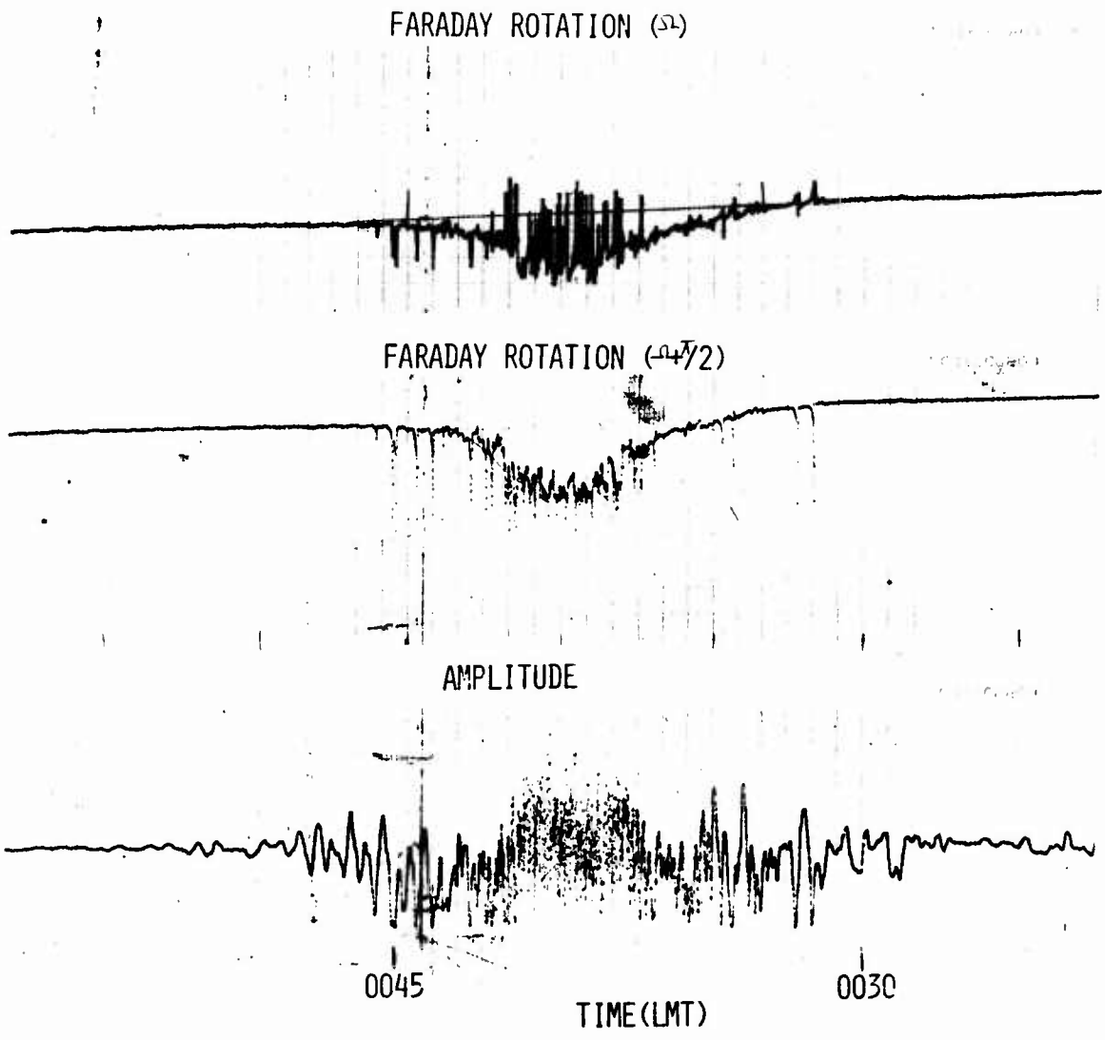

Fig. 4. Original record for November 16, 1978, from Natal (5.9°S, 35.2°W) using 136-MHz transmissions from satellite SMS 1 (90°W) showing the occurrence of an isolated bubble and its accompanying increases in the scintillation index, the average amplitude, and the fading rate.

Isolated Depletions and Enhancements in TEC

The recent measurements at the magnetic equator have helped to reach some understanding about the nature of one kind of ionospheric perturbation occurring at night. Such perturbations are described variously as ionization depletions, bubbles, plumes, and some type of irregularity patches, or equatorial spread *F* irregularities. On the experimental side the radar backscatter maps [*Woodman and LaHoz*, 1976] show dramatically the plumelike structures when they are viewed vertically upward as a function of time at a fixed location. In in situ measurements, large depletions of ionization are observed as the satellite passes nearly horizontally [*McClure et al.*, 1977] or as the rocket traverses nearly vertically [*Kelley et al.*, 1976] through these bubbles. On the basis of propagation measurements the occurrence of these bubbles has been shown to be correlated with the onset of scintillation on satellite radio signals [*Aarons*, 1977; *Basu and Basu*, 1976]. These have also been found to be responsible for backscattering in transequatorial propagation [*Röttger*, 1976]. On the theoretical side, early investigations have shown that the bottomside ionosphere is subject to Rayleigh-Taylor instabilities [*Liu and Yeh*, 1966*a*, *b*]. Recent numerical simulations have shown that as the depletion increases, the nonlinear polarization $\mathbf{E} \times \mathbf{B}$ forces in the equatorial geometry can drive the depleted region upward through the ionization peak to the topside ionosphere [*Ossakow et al.*, 1979].

Yeh et al. [1979*a*, *b*] reported observations of ionospheric bubbles utilizing the 136-MHz Faraday rotation records from Natal, and *Wernik* [1979] presented a simple model of an equatorial bubble. Looking again at Figure 3, it may be noted

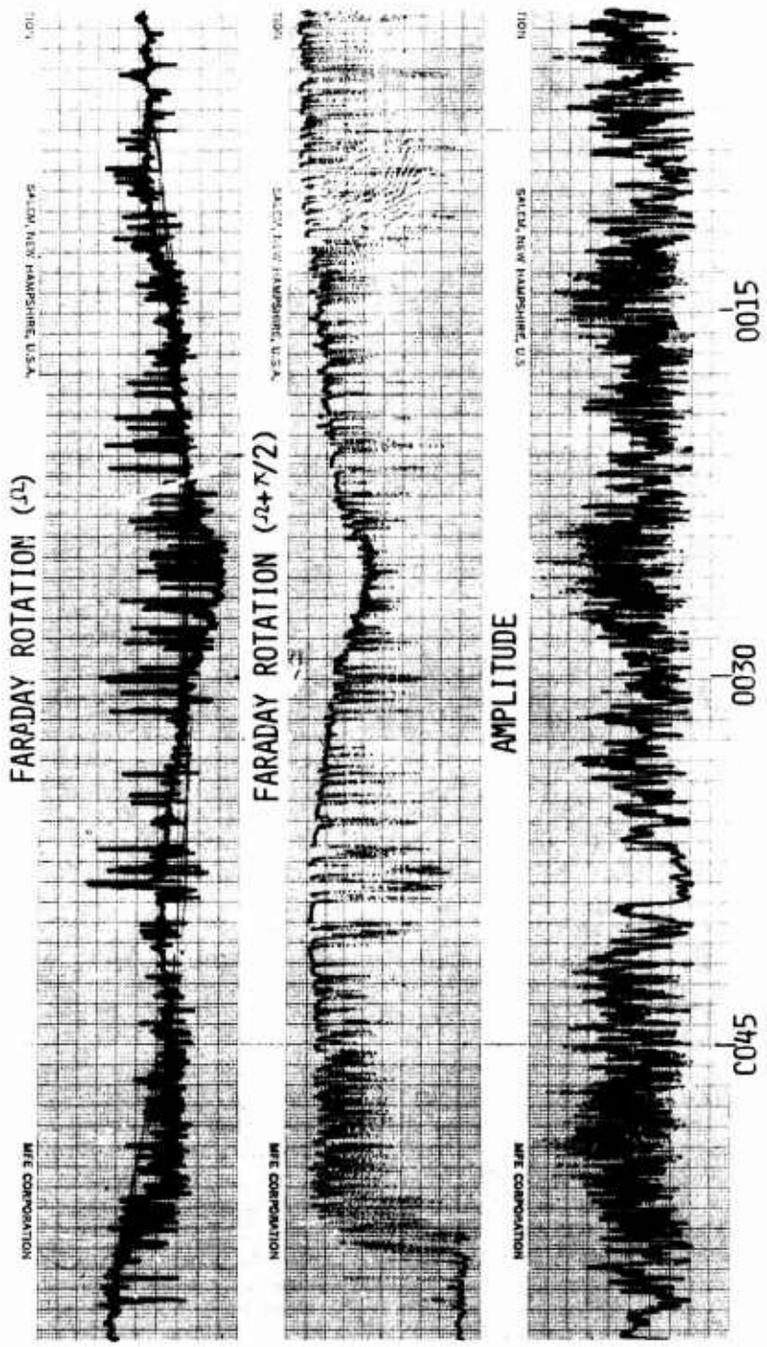

Fig. 5. Original record for November 12, 1978, from Natal using SMS 1 transmissions showing both enhancements and depletions in Faraday rotation. Note the characteristic behavior that the depletions are accompanied by increases in fading rate, scintillation index, and amplitude level, while the enhancements are accompanied by decreases in fading rate, scintillation index, and amplitude level.

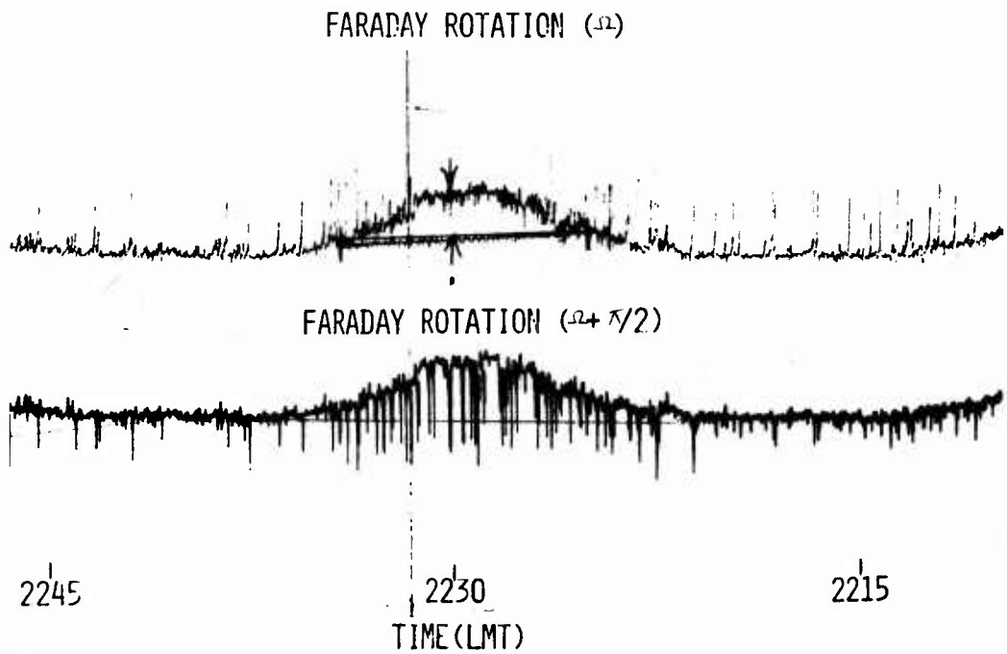

Fig. 6. Original record for September 19, 1978, from Natal using SMS 1 transmissions, showing an isolated enhancement.

that there are several sharp structures superposed over the background TEC variation. The first sharp depletion occurred at 1920 LMT, shortly after the onset of scintillations. There are also other depletions, but those occurring before local midnight are not as isolated and distinct as those occurring near or after midnight. For example, the bubble occurring at 0040 LMT on November 16, 1978, appeared in the original record as shown in Figure 4. Note the coincident increase in scintillation index as well as scintillation rate and the average amplitude level with the appearance of the bubble. This suggests that the isolated rapid scintillation rate can be used as a possible indicator of a bubble. It may be mentioned here that these isolated bubbles should not be taken as traveling ionospheric disturbances (TID), which generally have quasi-periodic and wavelike structure. It is very clear from Figure 3 that the five sharp depletions occurring successively a few hours around local midnight do not possess the usual TID appearance.

Another example is shown in Figure 5. The amplitude channel at the bottom shows rapid fluctuations at three times: near 0015, 0025, and 0050 LMT. Coincidentally, the depletions in Faraday rotation angle can be clearly identified for the latter two times but not so clearly for the former time. Every time the average amplitude level also shows an increase. In addition to sudden increases in scintillation rate, there are also times when scintillation rate is reduced momentarily and the average amplitude level is simultaneously decreased, coinciding with the increase in Faraday rotation angle. Two such cases can be identified in Figure 5, at 0010 and 0038 LMT. The labeling of Faraday rotation enhancement cases may look subjective, especially when they occur along with depletions as in Figure 5. Such doubts may be further reinforced from the fact that the in situ data have clearly shown the presence of isolated depletions in electron density, but no enhancement cases have been reported so far. However, the decrease in scintillation rate and scintillation index below the normal level at the time of enhancement and the rare example of isolated enhancement like the one shown in Figure 6 make us believe that both depletions and enhancements do occur, though their relative occurrence may be affected by the subjective approach. Consequently, the typical behavior of these events is as follows: The depletions in TEC are usually accompanied by simultaneous increases in fading rate, scintillation index, and the average amplitude level, while the enhancements in TEC are accompanied by simultaneous decreases in fading rate, scintillation index, and the average amplitude level. During the 1-year period from September 1978 through August 1979 a total of 990 cases consisting of 710 isolated depletions and 280 enhancements have been identified. Thus the cases of enhancements were only about 28% of the total cases. The statistics of these cases follows.

Figure 7 is a histogram showing the occurrence of isolated depletions and enhancements during different months for the period September 1978 to August 1979. It is clear that the occurrence of both depletions and enhancements is a maximum in the month of October and a minimum in August. It is noted that 67% of depletions occur during October–December and 80% during the period September–February, while 83% of enhancements occur during September–December. Furthermore, only 2% of depletions and 4% of enhancements occur during the May–August period. Figure 8 shows

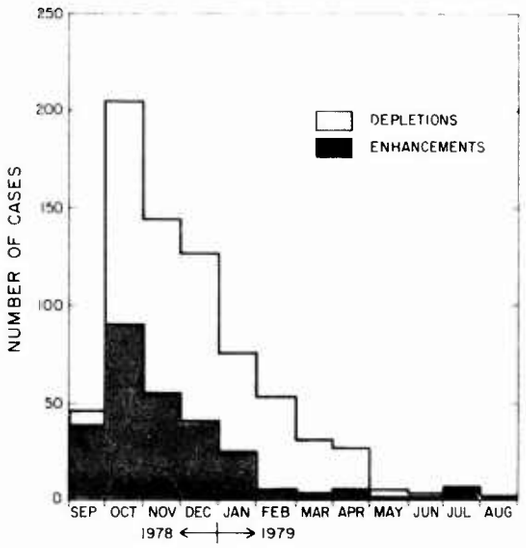

Fig. 7. Histogram showing occurrence of isolated depletions and enhancements during different months for the 1-year period from September 1978 to August 1979.

a histogram depicting the diurnal variation of the occurrence of such cases. It is clear that these depletions/enhancements occur mostly at night, between 1900 and 0300 LT, with a maximum between 2000 and 2300 LT.

A histogram depicting the duration of the ionization depletions/enhancements is given in Figure 9. Most of these cases last less than 20 min, with a large number of depletion cases (165) having a duration between 8 and 10 min, but there are also a number of depletions/enhancements lasting longer than half an hour. These depletions/enhancements have a distribution shown in Figure 10. Most of the cases have a decrease/increase in equivalent vertical electron content of less than 4×10^{16} el/m^2, but depletions as large as 1.2×10^{17} el/m^2 have also been observed, which is about 11–17% of the total diurnal change in TEC for the period October–December, when most of the cases occur.

Modeling of the Ionospheric Bubble

In an attempt to simulate a bubble by a model a Gaussian lateral distribution of electron density has been used. Assuming that the lateral distribution and the height distribution enter in a multiplicative manner, the two-dimensional electron density can be expressed as

$$N(x, h) = f(h) \cdot [1 - \alpha \exp - [(x - x_0)/l]^2] \qquad (1)$$

where

- h height;
- x lateral distance;
- α constant, usually smaller than unity;
- l half width of the bubble;
- $f(h)$ height distribution of the electron density of the background ionosphere.

Equation (1) gives an electron density model which represents a depletion when the constant α is positive and an enhancement when α is negative. In each case the maximum deviation occurs when $x = x_0$. When ray bending is ignored, the optical path ψ can be evaluated by the integration

$$\psi = \int n\, dh \cong \psi_0 - \frac{40.3}{f^2} \cdot N_{TB}[1 - \alpha \exp - [(x - x_0)/l]^2] \qquad (2)$$

where

- n refractive index;
- ψ_0 reference phase;
- N_{TB} background TEC, equal to $\int f(h)\, dh$.

According to ray theory the phase variation (2) along the wave front will develop into an amplitude variation after propagating a distance. This amplitude variation as observed on the ground can be shown to be proportional to the integral [*Yeh and Liu*, 1972]

$$\exp\left(-\frac{1}{2}\int_0^S \frac{d^2\psi}{dx^2}\, ds\right) = \exp\left[\frac{40.3\alpha N_{TB} S}{f^2 l^2} \cdot \left(1 - \frac{2(x - x_0)^2}{l^2} \cdot \exp - [(x - x_0)/l]^2\right)\right] \qquad (3)$$

Equation (3) gives the amplitude variation on the ground. If the amplitude is measured in decibels, its variation is then

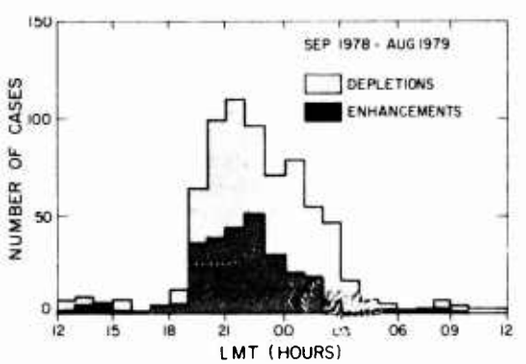

Fig. 8. Histogram showing the diurnal frequency of occurrence for the period September 1978 to August 1979.

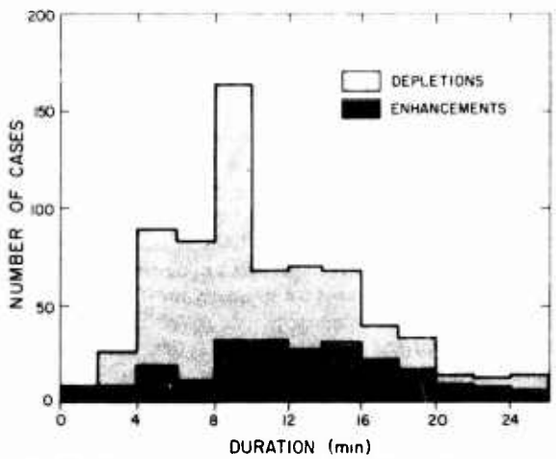

Fig. 9. Histogram showing the duration of ionization depletions and enhancements as observed along a fixed path for the period September 1978 to August 1979.

proportional to the exponent of (3). The parameters deduced from Figure 4 and used to calculate an amplitude pattern on the ground by using (3) are as follows:

$$\alpha = 0.163 \qquad f = 136 \text{ MHz}$$

$$N_{IB} = 3.5 \times 10^{17} \text{ el/m}^2 \qquad l = 18.5 \text{ km}$$

The bottom of the layer was assumed to be at a height of 300 km. Since the elevation angle is 28°, the path S turns out to be 640 km.

The calculated amplitude pattern on the ground is depicted in Figure 11. The similarity of the calculated and the experimentally observed average amplitude pattern is obvious. The maximum amplitude is dependent on the width of the bubble when the other parameters are fixed. In our case the best fit was achieved at $2l = 37$ km.

The minimum points of amplitude can be determined quite accurately from the observed amplitude variation (Figure 4). The time difference between the minima of the observed amplitude variation is approximately 450 s. The corresponding length in the calculated amplitude variation (Figure 10) is about 44 km, giving a drift velocity of about 98 m/s, which agrees well with drift velocities measured independently by other means [*Yeh et al.*, 1981].

As was pointed our previously, the amplitude pattern of enhancement can be computed simply by changing the sign of α in (1). On a logarithmic scale the curve will be the same shape as in the case of depletion, but turned upside down, because in (3), α is in the exponent. On a linear scale the nature of the curve will be different.

It is obvious that the suggested Gaussian model is not perfect. However, it describes quite well the main features of the average amplitude variation caused by the ionospheric bubble. The present model does not explain the change in fading rate and scintillation index caused by a bubble as described in the present work. This is because, in addition to a general depletion of electron density inside the bubble as modeled in (1), there are also sharp fingerlike wedges which are not contained in (1). Computations by *Wernik et al.* [1980] show that regions of sharp wedges can be sources of intense scintillations. The model constructed by them is based on in situ measurements [*McClure et al.*, 1977] and shows these highly complex structures with steep gradients in the center of the bubble. The horizontal gradients gradually decrease toward the edge of the bubble, as also revealed by in situ measurements. The computed pattern indicates an increase of the scintillation rate with increase of bubble thickness and shows a change in the scintillation rate with increase of bubble thickness and shows a change in the scintillation rate from slow, close to the edges of the bubble, to fast, at its center [*Wernik et al.*, 1980]. This is in complete agreement with our experimental results.

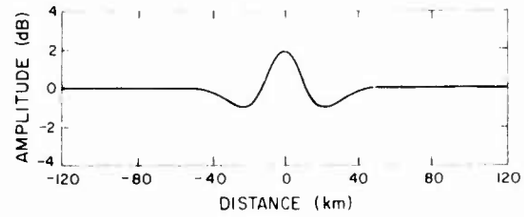

Fig. 11. Amplitude variation of a radio wave on the ground after passing through a bubble. The width of the bubble is 37 km, the frequency 136 MHz, and the distance from the layer 640 km. The estimated distance between the two minima is about 44 km.

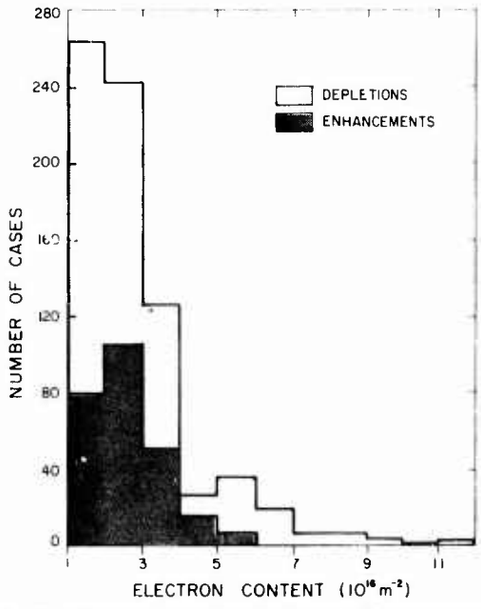

Fig. 10. Histogram showing the change in electron content for depletion and enhancement cases as observed during the period September 1978 to August 1979.

Acknowledgments. The authors wish to express their thanks to Francis J. Gorman for his assistance in installing the polarimeter operated at Natal. Thanks are also due to E. Bonelli and J. C. Carvalho for their assistance in making this experiment possible. This work was supported by the Center for Communication Systems, U.S. Army Communications and Research Command, under grant DAAB 07-80-M-6538, and the National Science Foundation under grant ATM 78-17846.

The Editor thanks J. P. McClure for his assistance in evaluating this paper.

REFERENCES

Aarons, J., Equatorial scintillations: A review, *IEEE Trans. Antennas Propagat.*, *AP-25*, 729, 1977.

Anderson, D. N., and R. G. Roble, The effect of vertical **E** × **B** ionospheric drifts on *F* region neutral winds in the low-latitude thermosphere, *J. Geophys. Res.*, *79*, 5231, 1974.

Anderson, D. N., and D. W. Rusch, Composition of the nighttime ionospheric F_1 region near the magnetic equator, *J. Geophys. Res.*, *85*, 569, 1980.

Basu, S., and S. Basu, Correlated measurements of scintillations and in-situ *F* region irregularities from Ogo-6, *Geophys. Res. Lett.*, *3*, 681, 1976.

Bittencourt, J. A., and Y. Sahai, Behaviour of the [OI] 6300Å emission at the magnetic equator and its relation to the vertical **E** × **B** plama drift velocity, *J. Atmos. Terr. Phys.*, *41*, 1233, 1979.

Bittencourt, J. A., and B. A. Tinsley, Tropical *F* region winds from O I 1356 Å and O I 6300 Å, *J. Geophys. Res.*, *81*, 3781, 1976.

Donatelli, D. E., P. M. Walsh, R. S. Allen, and J. A. Klobuchar, Enhancements and sharp depletions of TEC in the nighttime equatorial ionosphere, paper presented at Symposium on the Effect of the Ionosphere on Radiowave Systems, Nav. Res. Lab. and Air Force Geophys. Lab., Alexandria, Va., April 14–16, 1981.

Hunter, A. N., Faraday rotation of the 136 MHz transmission from geostationary satellite "Canary Bird" observed at Nairobi, *Radio Sci.*, *4*, 811, 1969.

Kelley, M. C., G. Haerendel, H. Kappler, A. Valenzuela, B. B. Balsley, D. A. Carter, W. L. Ecklund, C. W. Carlson, B. Havsler, and R. Torbert, Evidence of Rayleigh-Taylor type instability and upwelling of depleted density regions during equatorial spread *F*, *Geophys. Res. Lett.*, *3*, 448, 1976.

Koster, J. R., Equatorial scintillation, *Planet. Space Sci.*, *20*, 1999, 1972.

Koster, J. R., and T. Beer, An interpretation of ionospheric Faraday rotation observations at the equator, scientific report, Dep. of Phys., Univ. of Ghana, Legon, Accra, 1972.

Lanzerotti, L. J., C. G. Maclennan, and L. L. Cogger, Arecibo ionosphere TEC during nonstorm times, *J. Geophys. Res.*, *81*, 5573, 1976.

Liu, C. H., and K. C. Yeh, Low-frequency waves and gradient instabilities in the ionosphere, *Phys. Fluids*, *9*, 1407, 1966*a*.

Liu, C. H., and K. C. Yeh, Gradient instabilities as possible causes of irregularities in the ionosphere, *Radio Sci.*, *1*, 1283, 1966*b*.

McClure, J. P., W. B. Hanson, and J. H. Hoffman, Plasma bubbles and irregularities in the equatorial ionosphere, *J. Geophys. Res.*, *82*, 2650, 1977.

Ossakow, S. L., S. T. Zalesak, and B. E. McDonald, Nonlinear equatorial spread *F*: Dependence on altitude of the *F* peak bottomside background electron density gradient scale length, *J. Geophys. Res.*, *84*, 17, 1979.

Rishbeth, H., Polarization fields produced by winds in the equatorial *F* region, *Planet. Space Sci.*, *19*, 357, 1971.

Rishbeth, H., Dynamics of the equatorial *F*-region, *J. Atmos. Terr. Phys.*, *39*, 1159, 1977.

Röttger, J., The macroscale structure of equatorial irregularities, *J. Atmos. Terr. Phys.*, *38*, 97–102, 1976.

Wernik, A. W., Model computations of radio wave scintillation caused by equatorial bubbles, *Sci. Rep. 1*, Dep. of Electr. Eng., Univ. of Ill., Urbana, 1979.

Wernik, A. W., C. H. Liu, and K. C. Yeh, Model computations of radio wave scintillation caused by equatorial ionospheric bubbles, *Radio Sci.*, *15*, 559, 1980.

Woodman, R. F., and C. LaHoz, Radar observations of *F* region equatorial irregularities, *J. Geophys. Res.*, *81*, 5447, 1976.

Yeboah-Amankwah, D., and J. R. Koster, Equatorial Faraday rotation measurements on the ionosphere using a geostationary satellite, *Planet. Space Sci.*, *20*, 395, 1972.

Yeh, K. C., and C. H. Liu, *Theory of Ionospheric Waves*, pp. 228–237, Academic, New York, 1972.

Yeh, K. C., H. Soicher, C. H. Liu, and E. Bonelli, Ionospheric bubbles observed by the Faraday rotation method at Natal, Brazil, *Geophys. Res. Lett.*, *6*, 473, 1979*a*.

Yeh, K. C., H. Soicher, and C. H. Liu, Observations of equatorial ionospheric bubbles by the radio propagation method, *J. Geophys. Res.*, *84*, 6589, 1979*b*.

Yeh, K. C., C. H. Liu, J. P. Mullen, and E. Bonelli, The behaviour of scintillation at Natal in 1978, in *Scientific and Engineering Uses of Satellite Radio Beacons, Proceedings of the COSPAR/URSI Symposium*, pp. 259–263, Polish Scientific Publishers, Warsaw, 1981.

(Received June 15, 1981;
revised December 28, 1981;
accepted December 30, 1981.)